Origins of Nonstoichiometry and Vacancy Ordering in $Sc_{1-x}\square_xS$

Gus L. W. Hart and Alex Zunger
National Renewable Energy Laboratory, Golden, Colorado 80401
(Received 13 August 2001; published 13 December 2001)

Whereas nearly all compounds A_nB_m obey Dalton's rule of integer stoichiometry (n:m, both integer), there is a class of systems, exemplified by the rocksalt structure $Sc_{1-x}\square_xS$, that exhibits large deviations from stoichiometry via vacancies, even at low temperatures. By combining first-principles total energy calculations with lattice statistical mechanics, we scan an astronomical number of possible structures, identifying the stable ground states. Surprisingly, all have the same motifs: (111) planes with (112) vacancy rows arranged in (110) columns. Electronic structure calculations of the ground states (identified out of $\sim 3 \times 10^6$ structures) reveal the remarkable origins of nonstoichiometry.

DOI: 10.1103/PhysRevLett.87.275508 PACS numbers: 61.72.–y, 61.43.–j, 71.15.–m, 71.23.–k

While random $A_{1-x}B_x$ alloys made of mutually soluble elements can be entropically stabilized at sufficiently elevated temperatures in almost arbitrary stoichiometric ratios, nearly two centuries ago Dalton [1] discovered that almost all compounds A_nB_m occur in precise integer stoichiometry (n, m). The existence of such integer stoichiometry forms the centerpiece of Lewis' theory of valence [2] as it reflects the propensity of bonded atoms to donate, accept, or share an integer number of valence electrons with each neighboring atom. Although small deviations from precise stoichiometry are known to exist at finite temperatures due to intrinsic vacancies or interstitials, the formation of such defects costs energy, so their concentration is thermally activated. Yet there is a class of compounds that violate Dalton's rule in a big way, existing even at low temperatures in manifestly nonstoichiometric forms, with as much as 50% of their atoms missing [3–7]. Examples of such systems include transition metal oxides (TiO, VO), carbides and nitrides (TiC, HfN), and early transition metal chalcogenides (ScS, ZrSe, YS). We studied the paradigm nonstoichiometric system [8–12] $Sc_{1-x}\square_xS$, since it has the simple NaCl structure, exhibits vacancies (denoted by "□") on only one (metal) sublattice, shows a remarkable, unexplained series of vacancy-ordered structures at low temperatures extending to $Sc_2\square_1S_3$ (33% vacancies), and has been studied experimentally for a long time [8–12].

We wish to study how the electronic structure stabilizes such a remarkable range of nonstoichiometry and to predict the low temperature vacancy-ordered structures. Since the crystal structures involving nonstoichiometry are, for the most part, unknown experimentally and since their metal-to-vacancy sequence is unsuspected via the usual chemical experience, one cannot resort to the conventional approach of guessing a handful of intuitively selected trial vacancy structures [6,13]. Instead, we will use the cluster expansion method [14–16], in which a series of first-principles, local density approximation (LDA) total-energy calculations on arbitrary ordered Sc_mS_n superstructures is mapped onto a generalized Ising Hamiltonian where the spin variables correspond to the presence or absence of Sc on each site. Once the Hamiltonian is determined, efficient ground state search techniques [17] are used to identify in an unbiased manner the global minimum-energy lattice configurations, whereas finite-temperature Monte Carlo simulations are used to study order-disorder phase transitions. Having identified a handful of $T = 0$ *ground states* (out of $\sim 3 \times 10^6$ possible candidate structures), we study their electronic structure via the LDA pseudopotential approach, finding the electronic origins of their stabilized nonstoichiometry. We find that the electronic structure of the ground state configurations exhibits a remarkable "self-regulating response" (SRR) [18] mechanism which stabilizes these structures: although removal of Sc atoms from the lattice reduces the number of d electrons, these electrons are taken away from energetically unfavorable, antibonding states. But more importantly, the system responds to the extraction of (antibonding) electrons by replenishing d charge to the bonding orbital. This restores to the neighborhood of the remaining Sc atoms much of the d charge removed via vacancy formation and stabilizes the structure.

The cluster expansion (CE) expresses the excess energy of any lattice configuration σ [a particular occupation of the N lattice sites by A or B atoms ($S_i = +1$ or -1, respectively)] as

$$\Delta H_{\mathrm{CE}}(\sigma) = J_0 + \sum_f^{N_f} D_f \overline{\Pi}_f(\sigma) J_f \,, \qquad (1)$$

where J_f is the effective atom-atom interaction for cluster type f (pair, triangle, tetrahedron, etc.), N_f is the number of clusters of type f in configuration σ, D_f is the number of clusters of type f per lattice site, and $\overline{\Pi}_f$ are the averaged spin products [15] for configuration σ. In the case of $Sc_{1-x}\square_xS$, the up and down "spins" represent the scandium atom and its vacancy, respectively. Because it is present on every anion site and does not constitute a configurational degree of freedom, the sulfur atom is not explicitly included in the expansion (but it is included, of course, in the LDA calculations of the total energy). The

J's are determined by fitting the expansion $\Delta H_{\mathrm{CE}}(\sigma)$ to the excess total energies $\Delta H_{\mathrm{LDA}}(\sigma)$ of a set of N_σ "input structures" calculated by first-principles methods. We use the pseudopotential plane wave method [19], as implemented in the VASP code [20]. In each case, we relax both cell-external and cell-internal degrees of freedom to obtain $\Delta H_{\mathrm{LDA}}(\sigma)$. The interactions were chosen by first eliminating from the fit several of the input structures and choosing the interactions that result in an accurate fit to the structures retained as well as accurate predictions for the eliminated structures. The process is repeated [21] using different sets of eliminated structures to ensure a set of interactions that work well *generally*. In the case of ScS, a very robust fit was obtained with 25 pair and 7 three-body and four-body interactions. Typical fitting and prediction errors for ScS are ~ 9 meV/atom, whereas the average ΔH is approximately -500 meV/atom. In the simulations discussed below, we used a final fit that included all 31 of the input structures.

Once the CE has been constructed so that the formation enthalpy of arbitrary configurations of many atoms can be quickly evaluated, the $T = 0$ ground state configurations at different vacancy concentrations are easily determined. Two approaches can be used: (i) direct enumeration [17] and (ii) "simulated annealing" Monte Carlo searching. Our implementation of direct enumeration tries *every* possible configuration subject to the restriction that none of the candidate configurations contains more than 20 atoms per primitive cell. There are approximately 3.1×10^6 such configurations for the fcc lattice. Simulated annealing uses a large simulation cell and slowly "cools" the simulation cell, selecting configurations via a Monte Carlo approach. The two approaches are complementary and together yield a powerful tool for determining ground states. Figure 1 shows the results of a ground state search via direct enumeration. The ground states are shown as circles connected by a convex-hull line. These circles correspond to structures that are the absolute stable forms with respect to both other structures at the same composition and with respect to phase separation into structures of neighboring compositions. Note that, unlike the case for conventional alloys such as $Cu_{1-x}Au_x$, there are low-energy excited configurations at most compositions. The most stable structure is at $x = 1/3$. The direct enumeration method identifies 12 ground states for $0 < x \leq 1/3$ (the physically relevant composition range). Several of these are visualized in Fig. 2. Analysis of the identified ground state structures reveals the following common features.

Local coordination chemistry.—The NaCl structure of ScS is built from S-centered Sc_6 octahedra. We find that each octahedron can have 0, 1, or 2 vacancies, but no more; i.e., the number of vacancies per octahedon is as small as possible for a given concentration. So, the structure at $x = 1/6$ has exactly one vacancy per octahedron, whereas the structure $Sc_2\square_1S_3$ ($x = 1/3$) has exactly two vacancies in every octahedron. In all cases of divacant octahedra, the vacancies are nearest neighbors (i.e., lie on the same face of the octahedron). This means that *cis*, not *trans* (vacancies on opposite corners of the octahedra), arrangements are energetically favored. This is consistent with Burdett's observation [6] that no known inorganic solids have square-planar coordinated sulfur atoms. In our Monte Carlo simulations, we find *trans*-divacant octahedra are quickly replaced by *cis*-divacant octahedra because the vacancies arrange themselves to avoid square-planar coordination. This is true even for somewhat disordered configurations. Additionally, we find (from LDA calculations) that the average bond length for the low-energy structures decreases by less than 0.4% over the range $0 < x \leq 1/3$ indicating that the underlying NaCl lattice

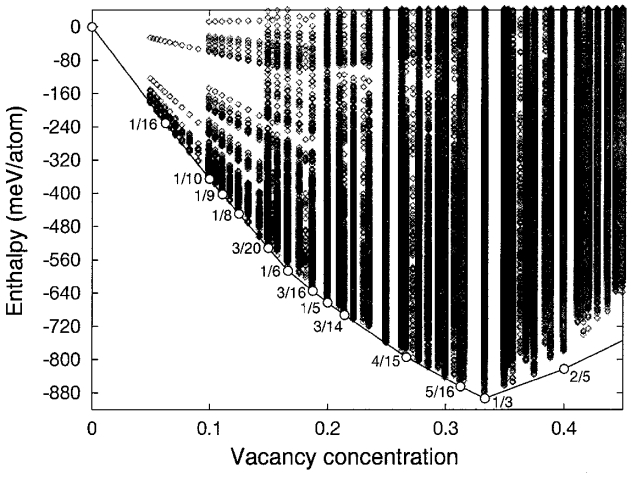

FIG. 1. Total formation energies of $\sim 3 \times 10^6$ structures (denoted by diamonds) of $Sc_{1-x}\square_xS$ obtained from the LDA-fitted cluster expansion, showing the 12 ground state structures (open circles) for $x \leq 1/3$.

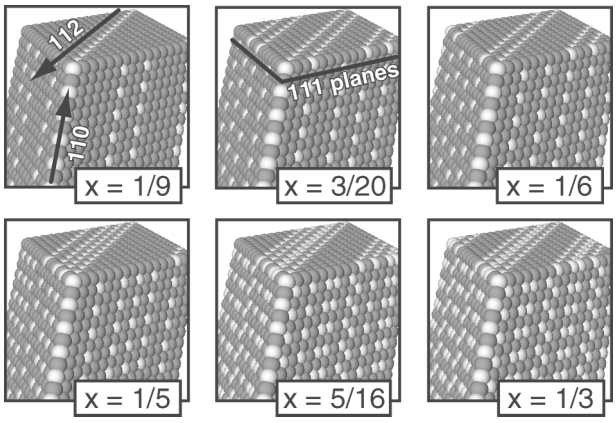

FIG. 2. Crystal structures of 6 of the 12 ground states (see Fig. 1) of $Sc_{1-x}\square_xS$. Dark spheres are Sc atoms, and white spheres are Sc vacancies (sulfur atoms are not shown). Note the existence of (111) planes which contain (112) atomic rows. The stacking arrangement of (111) planes is such that the (112) rows form (110) columns of alternating vacancies. The ground state structures can be characterized by their (112) row sequence (Table I).

is essentially undisturbed by the introduction of vacancies, as seen in x-ray studies [8,23].

Long range order.—There are three central features common to all but one ground state structure. We find (Fig. 2) the following: (i) Repeat plane: the basic plane that repeats periodically is (111). (ii) Vacancy rows: within the (111) plane, we find that vacancies form (112) rows. For example, at $x = 1/6$ the rows form the in-plane sequence $V_1M_2V_1M_8$ [i.e., two vacancy rows (V) are separated by two adjacent metal rows (M), then by eight], whereas at $x = 1/3$ the rows form the in-plane sequence $V_1M_1V_2M_1V_1M_6$. Similar patterns are seen at all other concentrations except $x = 4/15$. (iii) Vacancy columns: the (111) planes are stacked such that the (112) rows form vertical (110) alternating-vacancy columns. Within such columns every second site is a vacancy.

Our results agree with experiment regarding the existence of (111) repeat planes, and a (112) vacancy-row motif, seen experimentally in one case $x \simeq 0.20, T \simeq 300$ °C [9]. We find, however, that this is a general motif common to all ground states. Experiment further finds for $x \simeq 0.20$ and $x \simeq 0.31$ that the (111) planes alternate with two different in-plane compositions. We find this to be the case for $x = 3/20$ (15%) and for $x = 5/16$ (~31%). However, at $x = 5/16$, the existence of an alternating concentration in the (111) planes occurs only at finite temperatures (in Monte Carlo simulations) but is remarkably similar to the results seen by Dismukes [8] for concentrations near $1/3$. The predicted structure of the most stable, $Sc_2\square_1S_3$ phase (see Table I) agrees perfectly with experiment [8].

We have solved the finite-temperature cluster-expansion Hamiltonian of Eq. (1) via Monte Carlo simulations, finding the order-disorder transition temperatures (Table I) for each of the ground states. We predict that T_c increases more or less monotonically with vacancy concentration, a surprising trend explained below.

TABLE I. Sequence of (112) rows in each (111) plane for the ground state structures $0 < x \leq 1/3$ and order-disorder transition temperatures T_c for each structure. Estimated error in T_c, ±5%. (V is a vacancy row; M is a filled row.)

Ground state	x	T_c (K)	(112) Row sequence
1	1/16	290	V_1M_{15}
2	1/10	400	$V_1M_2V_2M_{16}$
3	1/9	610	$V_1M_2V_1M_{14}$
4	1/8	950	$V_1M_2V_1M_{12}$
5	3/20	1100	$V_1M_2V_1M_6$ (first layer) V_1M_9 (second layer)
6	1/6	1360	$V_1M_2V_1M_8$
7	3/16	1405	$V_1M_2V_1M_1V_1M_{10}$
8	1/5	1390	$V_1M_2V_1M_1V_1M_1V_1M_{12}$
9	3/14	1320	$V_1M_1V_1M_1V_1M_9$
10[a]	4/15	1960	$V_1M_1V_1M_4V_1M_1V_1M_5$
11	5/16	2890	$V_1M_1V_1M_1V_2M_1V_1M_8$
12	1/3	3050	$V_1M_1V_2M_1V_1M_6$

[a](110) rows instead of (112) rows.

Once we know the ground state structures, we can study the electronic origins of nonstoichiometry by performing band structure calculations on the identified ground states. Previous attempts to explain nonstoichiometry [6,13,24] did not have access to the low-energy configurations. We find that the well known models (localized states, defect clusters, etc.) [7,25] for nonstoichiometric binary oxides are inapplicable to ScS. Figure 3 shows the densities of states for the two limiting cases: ScS (no vacancies) and $Sc_2\square_1S_3$ (33% vacancies). The results for intermediate x structures lie in between these two extremes. In the stoichiometric NaCl structure of ScS (Fig. 3) we find, in agreement with previous calculations [6,13], a fully occupied metal bonding d band, hybridized with a fully occupied nonmetal p band. Just below the Fermi level we have the partially occupied metal antibonding d band. In stoichiometric ScS, the bonding and antibonding d bands are each occupied by one-half electron per scandium atom. As metal vacancies form, the Fermi energy moves to lower values, thus emptying the antibonding d band. Naively, one would assume that these will transition from Sc^{2+} d^1 towards Sc^{3+} d^0. However, in reality, such a large change in oxidation state is avoided through a "self-regulating response" mechanism [18]. The numbers inscribed next to the densities of states traces in Fig. 3 denote the number of electrons per scandium atom in each band. We see that while $0.5e$ are lost from the antibonding Sc d state upon forming $1/3$ vacancies per cell, the Sc d bonding band

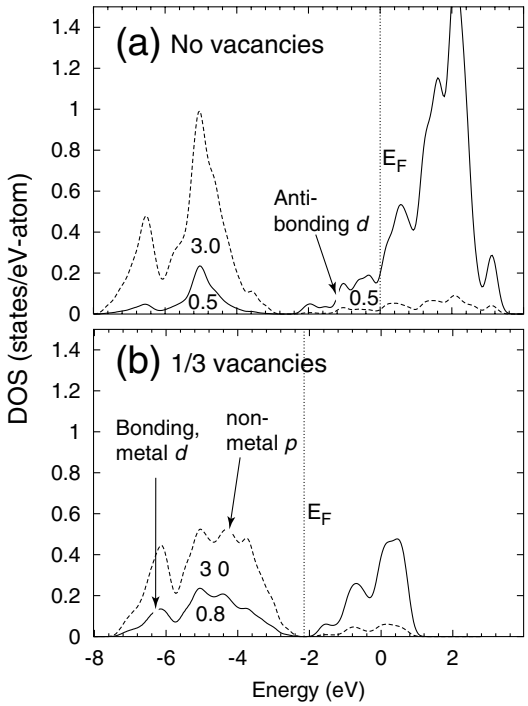

FIG. 3. Partial DOS of stoichiometric ScS (a) and 33% nonstoichiometric $Sc_2\square_1S_3$ (b). The numbers indicate the number of electrons in each band. Note that while charge is lost from the antibonding band upon vacancy formation, the metal bonding state gains charge.

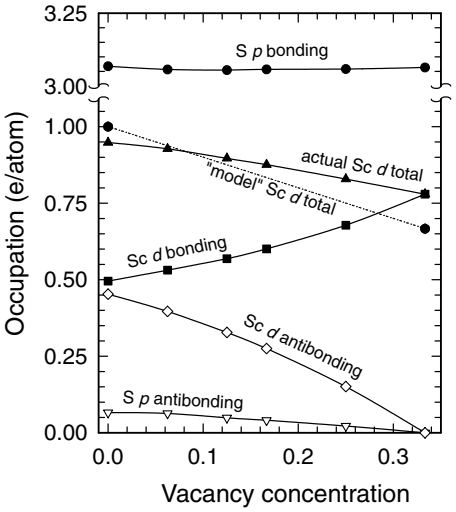

FIG. 4. Band-by-band electron occupations as a function of vacancy concentration. "Model" Sc d refers to what the Sc d-band occupation would be if no rehybridization occurred.

increases its charge through rehybridization from $0.5e$ to $0.8e$. Thus, only $0.2e$ are actually lost from the Sc site upon forming $1/3$ vacancies/cell. Figure 4 shows these integrated band-by-band charges for the full range of nonstoichiometry. We see that the actual Sc d charge is reduced only moderately as vacancies form, since the large depletion of Sc d antibonding charge is offset by an almost equally large increase in the Sc d bonding charge (the sulfur s and p bands are almost unaffected). The metal d bonding charge *increases* with vacancy concentration, reaching its highest value for $Sc_2\square_1S_3$. This trend is reflected by the increase of T_c with x (Table I). The stabilization of metal vacancies through the emptying of metal antibonding d states and rehybridization of bonding states is expected to exist so long as the antibonding band is less that half occupied. How general is this effect? In cases where there are more than two d electrons in the antibonding band, the mechanism is suppressed, and, in fact, the NaCl structure itself is no longer stable. The mechanism also is inoperable if the d band is empty. Indeed, we find positive formation enthalpies for vacancies in d^0 compounds such as CaS, CaSe, etc. Thus, this mechanism explains nonstoichiometry in d^1 and d^2 chalcogenides such as ScS, ScSe, ZrS, etc., or lack of nonstoichiometry in d^0 chalcogenides such as CaS, CaSe, etc.

In summary, we have elucidated the mechanism for forming vacancies and predicted the lowest energy ordered-vacancy states for ScS. The fact that mechanism applies generally to early transition-metal chalcogenides explains the nonstoichiometry observed in these related compounds. The cluster expansion method can also be applied to these related materials as well to predict the ground state structures and ordering trends which are not well known experimentally.

This work was supported by the U.S. Department of Energy, DOE-SC-BES-DMS under Contract No. DE-AC36-00-GO10337.

[1] J. Dalton, *A New System of Chemical Philosophy* (R. Bickerstaff, Manchester, 1808).
[2] G. N. Lewis, *Valence* (The Chemical Catalog Company, New York, 1923).
[3] *Chemistry of Nonstoichiometric Compounds,* edited by K. Kosuge (Oxford University Press, Oxford, 1994).
[4] *Nonstoichiometric Oxides,* edited by O. T. Sorenson (Academic Press, New York, 1981).
[5] *Non-Stoichiometric Compounds,* edited by L. Mandelcorn (Academic Press, New York, 1981).
[6] J. K. Burdett and J. F. Mitchell, Prog. Solid State Chem. **23**, 131 (1995); Chem. Mater. **5**, 1465 (1993).
[7] R. Collongues, Prog. Cryst. Growth Charact. **25**, 203 (1992).
[8] J. P. Dismukes and J. G. White, Inorg. Chem. **2**, 1220 (1964).
[9] H. F. Franzen, R. T. Tuenge, and L. Eyring, J. Solid State Chem. **49**, 206 (1983).
[10] H. Hahn, The Chemical Society Special Publication **12**, 263 (1958).
[11] H. F. Franzen and J. C. W. Folmer, J. Solid State Chem. **51**, 396 (1984).
[12] A. R. Moodenbaugh, C. C. Johnston, R. Viswanathan, R. N. Shelton, L. E. DeLong, and W. A. Fertig, J. Low Temp. Phys. **33**, 175 (1978).
[13] D. K. Misemer and J. F. Nakahara, J. Chem. Phys. **80**, 1964 (1984).
[14] A. Zunger, in *Statics and Dynamics of Alloy Phase Transitions,* NATO ASI (Plenum Press, New York, 1994).
[15] L. G. Ferreira, S.-H. Wei, and A. Zunger, Phys. Rev. B **40**, 3197 (1989).
[16] J. M. Sanchez, F. Ducastelle, and D. Gratias, Physica (Amsterdam) **128A**, 334 (1984).
[17] L. G. Ferreira, S.-H. Wei, and A. Zunger, Int. J. Supercomput. Appl. **5**, 34 (1991).
[18] U. Lindefelt and A. Zunger, Solid State Commun. **45**, 343 (1983).
[19] J. Ihm, A. Zunger, and M. Cohen, J. Phys. C **12**, 4409 (1979).
[20] G. Kresse and J. Furthmüller, Phys. Rev. B **54**, 11 169 (1996); Comput. Mater. Sci. **6**, 15 (1996).
[21] The fit is optimized by requiring the "maximum smoothness criteria" (Eqs. 24–26 of Ref. [24]). The parameters t and λ are simultaneously optimized to yield both a good fit for fitted structures and accurate predictions for "eliminated" structures.
[22] D. B. Laks, L. G. Ferreira, S. Froyen, and A. Zunger, Phys. Rev. B **46**, 12 587 (1992).
[23] R. T. Tuenge, F. Laabs, and H. F. Franzen, J. Chem. Phys. **65**, 2400 (1976).
[24] H. F. Franzen, *Physical Chemistry of Inorganic Crystalline Solids* (Springer-Verlag, Berlin, 1986).
[25] J. B. Goodenough, Prog. Solid State Chem. **5**, 145 (1972).